Research Article

Optical haze of transparent and conductive silver nanowire films

Colin Preston[1], Yunlu Xu[2,3], Xiaogang Han[1], Jeremy N. Munday[2,3], and Liangbing Hu[1] (✉)

[1] *Department of Materials Science and Engineering, University of Maryland, College Park, College Park, Maryland 20742, USA*

[2] *Department of Electrical and Computer Engineering, University of Maryland, College Park, Maryland 20742, USA*

[3] *The Institute for Research in Electronics and Applied Physics, University of Maryland, College Park, Maryland 20742, USA*

ABSTRACT

Contemporary nanostructured transparent electrodes for use in solar cells require high transmittance and high conductivity, dictating nanostructures with high aspect ratios. Optical haze is an equally important yet unstudied parameter in transparent electrodes for solar cells that is also determined by the geometry of the nanostructures that compose the electrode. In this work, the effect of the silver nanowire diameter on the optical haze values in the visible spectrum was investigated using films composed of wires with either small diameters (~60 nm) or large diameters (~150 nm). Finite difference time domain (FDTD) simulations and experimental transmittance data confirm that smaller diameter nanowires form higher performing transparent conducting electrode (TCE) films according to the current figure of merit. While maintaining near constant transmittance and conductivity for each film, however, it was observed experimentally that films composed of silver nanowires with larger diameters have a higher haze factor than films with smaller diameters. This confirms the FDTD simulations of the haze factor for single nanowires with similarly large and small diameters. This is the first record of haze properties for Ag NWs that have been simulated or experimentally measured, and also the first evidence that the current figure of merit for TCEs is insufficient to evaluate their performance in solar cell devices.

1   Introduction

A transparent conducting electrode (TCE) acts as the top contact in a solar cell stack and is an important factor in determining the device efficiency. Optimal transparent electrodes must maintain a high conductivity in order to prevent ohmic dissipation of heat in the circuit and also maintain a high transparency in order to maximize the absorbed light in a solar cell's conversion layer. The most popular TCE materials to date are conducting metal oxides, such as indium tin oxide (ITO) [1]. ITO stands as the benchmark material because of its high conductivity (10 $\Omega \cdot$sq.$^{-1}$) and high transparency (90%) [2]; however, the high

cost of indium, the inherent brittleness of its ceramic structure, and its costly deposition technique render ITO inapplicable to low cost manufacturing and flexible solar modules [3]. Recent studies have suggested carbon nanotubes (CNTs) [4–7], grapheme [8–10], and metallic nanostructures [11–14] as compelling alternatives to ITO. Despite the high conductivity of individual metallic CNTs (~10^6 S·cm^{-1}) [15], the resistivity of CNT junctions in a nanotube network [2] and the bundling of nanotubes in a given CNT yield cause the sheet resistance of metallic CNT transparent electrodes at acceptable transparencies (80%–90%) to be too high (200–1,000 Ω·sq.$^{-1}$) [16, 17] for conventional use in solar cells. Graphene is a cheaper material than both CNTs and ITO; however, it does not exhibit a low enough resistance (~350 Ω·sq.$^{-1}$) [18] at acceptable transparencies (80%) for use in solar cells. Metallic nanowires are another alternative that exhibits high conductivity and optical transmittance in ordered and random networks [19–22]. Silver nanowire (Ag NW) TCEs are reported to compete with, and even surpass, the electrical and optical properties of ITO TCEs [11–13, 16, 22, 23]. Ag NW networks also benefit from cost efficient and scalable deposition techniques such as roll-to-roll printing [16], dry contact printing [12], and drop cast deposition [21]. The Ag NWs most pursued for TCEs exhibit a high aspect ratio [24]. Long wires with small diameters are reported to sustain a better electron percolation across the 2D network [7, 21] and enhanced transparent properties due to reduced coupling to surface plasmon resonances [13]. Therefore, most efforts in developing adequate Ag NW networks to replace ITO in TCEs aim at long wires with small diameters to achieve the highest transparency at the lowest sheet resistance.

The value of a TCE is quantified by a figure of merit that incorporates its critical properties into a single numerical relation. The figure of merit used for solid films [25] and nanostructure networks [2, 32, 33] reference the sheet resistance and the transparency of the electrode as the primary properties of merit affecting its function in a solar cell. Another critical property of a TCE is its haze factor, which is not currently considered in modern TCE designs [7, 26]. Haze refers to the degree of incident light scattered

forward towards the absorber layer, which enhances the path length of light and thus the short circuit current density of the solar cell. The magnitude of the light scattering in nanowire mesh TCEs is reported to be correlated with the geometry of the wire, in particular the diameter [13, 26]. While most reports indicate that large aspect ratios achieved by wires with small diameters and long lengths best optimize the performance of Ag NW TCEs, larger diameter wires have larger scattering cross-sections. To our knowledge this is the first study that elucidates the significance of haze in evaluating nanostructured TCE performance in solar cells, and calls into question the contemporary figure of merit for such TCEs. In this report, (1) the haze factor of small and large diameter individual Ag NWs was calculated and compared using finite difference time domain (FDTD) simulations, (2) the contemporary TCE figures of merit were compared for small and large diameter Ag NW TCE films, and (3) the haze factor of small and large diameter Ag NW TCE films with comparable sheet resistance and transparencies was experimentally measured and compared.

2   Results and discussion

2.1   Optical properties of silver nanowires—Theory

The scattering of individual nanowires is a logical starting point to launch further investigations into the light scattering of Ag NW TCEs. The scattering cross-section of individual cylindrical nanowires may be quantified through the theory proposed [27, 28] by Mie et al. Investigations into the scattering cross-sections of nanowires depicted by elliptical cylinders [29] and arbitrary cross-sections [30] have also been investigated. However, for more general cases it is often advantageous to solve Maxwell's equations numerically on a grid using FDTD simulations. This simulation method has been shown to be useful for investigating the optical transmittance properties of silver nanostructure transparent electrodes [13, 31]. The present work investigates the haze factor of Ag NWs with relatively large and small diameters theoretically through their scattering behavior projected by FDTD simulations (Fig. 1).
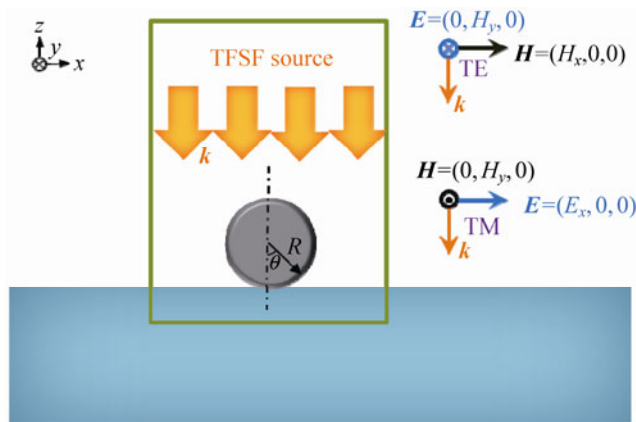
Figure 1 Schematic of the 2D simulation setup used to calculate the light scattering behavior at normal incidence from a single silver nanowire with a radius of *R*. The center of the nanowire is the origin of the axes. The green box represents a total field scattered field (TFSF) source with a length of 500 nm in the *x*-direction. The length is chosen according to the average spacing between Ag NWs as calculated from SEM images.

2.1.1 Evaluating haze factor

A cylindrical Ag NW with a large aspect ratio rests on a semi-infinite dielectric plane. A plane wave with either a TE or TM polarization (as defined in the inset) is incident on the nanowire from above and is perpendicular to the plane of the substrate. Monitors are put outside the total field scattered field source (the green box in Fig. 1) to detect the scattered power flux (Poynting vector) in order to get the forward scattered power (i.e., power that resides within an angle of 90° from the *z*-axis). The scattering cross-section is calculated to obtain the fraction of the forward propagating light that is not scattered. The

haze is defined as

$$
\text{Haze} = \frac{\text{Forward scattered light}}{\text{Forward nonscattered light} + \text{Forward scattered light}} \times 100\%
$$

(1)

2.1.2 Comparing haze factor to optical transmittance

The transmission, or percentage of incident light entered into the substrate, and haze factor for two Ag NWs diameters were simulated and compared in Fig. 2. The transmittance of the larger diameter nanowires is less than that of the smaller diameter nanowires by ⩽30% according to the average of the TM and TE polarization modes; however both large and small diameter transparencies are suitable for TCE utilization. Previous studies of the resistivity of individual silver nanowires [34] have shown that the conductivity does not vary between silver nanowires with these two diameters. Projecting these nanowire properties to a nanomesh film composed of each nanowire diameter, and referring to the current figure of merit that evaluates the performance of a TCE based on its electrical and transparent properties, the smaller diameter nanowires are more suitable for TCEs. The fact that optical haze is not considered when determining the performance of TCEs makes this conclusion flawed. Further analysis of the scattered field intensity with regards to the scattering angle from the silver nanowires shown in Fig. 3 demonstrates that for both TE and TM polarizations not only do the highest field intensities propagate forward rather than reflect backward, but relatively high intensities
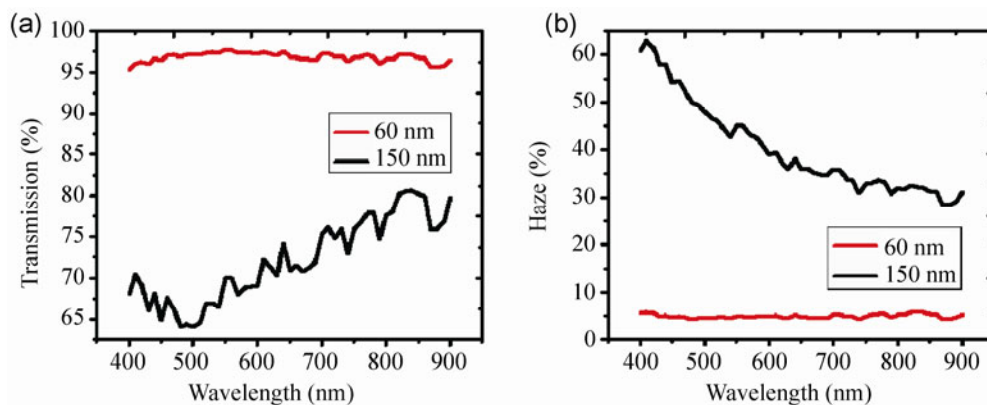

Figure 2 Simulation of (a) transmission and (b) haze factor of Ag NWs with different diameters (60 nm and 150 nm).
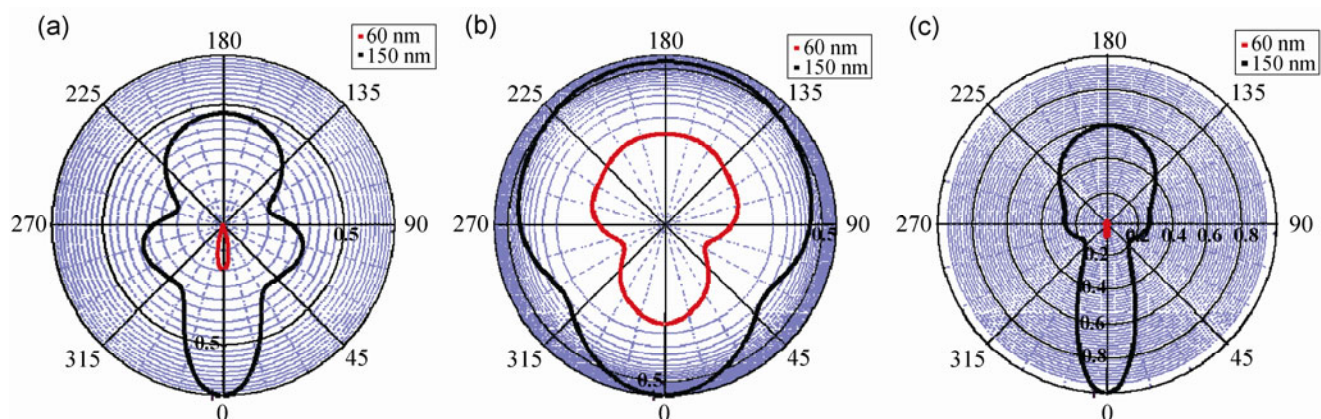
Figure 3 Simulation of the normalized scattered field intensity versus scattering angle from the axis normal to the silver nanowire with diffuse scattering represented by acute angles (0°–90° and 270°–360°) and backscattering represented by obtuse angles (90°–270°) for (a) TE polarization and (b) TM polarization and (c) average of TE and TM for 60 nm and 150 nm diameter silver nanowires. (a) and (b) are in log scale and (c) is in linear scale for clarity.

are measured for a range of forward angles (0°–90°). Because the forward scattered fields are not restricted to negligibly small angles, but expand to larger forward angles as well, the impact of diffuse scattered light must be addressed.

It is also clear from the simulations shown in Fig. 2 that the fraction of forward scattered light from forward propagated light increases as the nanowire diameter increases. At a wavelength of 500 nm, the haze factor is 40% higher for the larger diameter (150 nm) Ag NW, with the haze factor almost entirely disappearing just beyond the visible spectra for small diameters. If the transparency and sheet resistance of separate nanomesh films composed of small and large diameter Ag NW networks remain the same due to different wire concentrations, the greater haze factor for the larger diameter Ag NWs implies that TCEs that incorporate these nanowires greatly increase the path length in the conversion layer compared with devices that use TCEs with small diameter nanowires.

2.2 Optical measurements for silver nanowire transparent electrodes

In order to confirm that larger diameter nanowires may indeed form better performing nanomesh TCEs, films with equal transparencies and conductivities were fabricated from large and small diameter nanowire dispersions by controlling the concentrations of the nanowire dispersions before filtration. Large diameter

Ag NWs dispersed in ethanol were purchased commercially. Small diameter Ag NWs were synthesized using a slow titration method [23, 35]. The SEM images in Figs. 4(a) and 4(b) show an average radius of 60–70 nm and length of ~25 μm. The average diameter of the larger Ag NWs is ~150 nm and the average length is ~20 μm according to Figs. 4(c) and 4(d). It is clear from these images that there is high uniformity in length and diameter for both Ag NW dispersions, and there is minimal presence of nanoparticles in the films that may alter its sheet resistance. Ag NW films were transferred onto polydimethylsiloxane (PDMS) substrates via a vacuum filtration of dispersed nanowire dispersions on anodic aluminum oxide (AAO) filters. The sheet resistance of the Ag NW films was measured with a four-point probe, and the transmittance data was measured with a Lambda 35 UV/vis spectrometer. Films with various densities composed of either small or large Ag NW diameters are illustrated in Fig. 5, which displays the transmittance of the films or their transparency versus sheet resistance.

2.2.1 *Evaluating the contemporary figure of merit*

By altering the concentration of nanowires in each film, the distribution of Ag NW TCE films demonstrated in Figs. 5(a) and 5(b) was achieved. The relationship between the transmittance and sheet resistance for each TCE type (relatively small diameter and large diameter) was compared with the contemporary
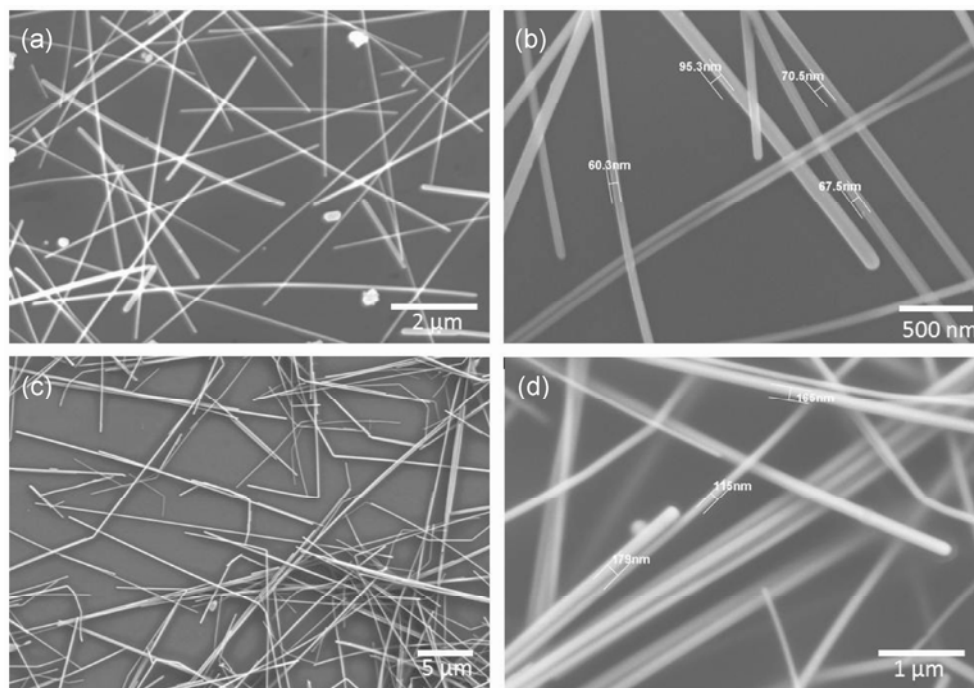
Figure 4 SEM images of Ag NWs: (a) percolation network of the film with small diameters; (b) display of small Ag NW diameters with little deviation, the diameters are as small as ~60 nm; (c) percolation network of film with large diameters; (d) display of large Ag NW diameters with little deviation, with an average of ~150 nm.
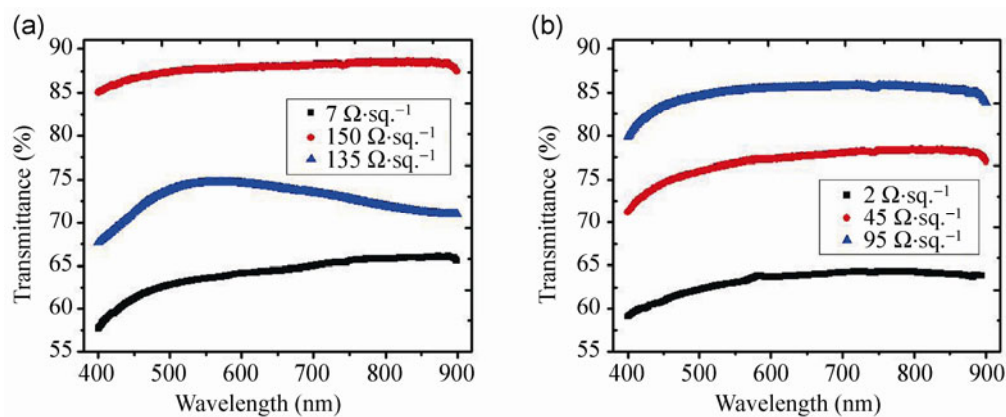

Figure 5 (a) The transmittance spectrum for the various films formed from vacuum filtration of Ag NW dispersions with large diameters (~150 nm). (b) The transmittance spectrum for the various films formed from vacuum filtration of Ag NW dispersions with small diameters (~60 nm).

figure of merit model [2, 7] for transparent electrodes composed of nanostructured films with a thickness below the percolation limit:

$$T\% = \left(1 + \frac{188.5}{R_s} \frac{\sigma_{\text{optical}}}{\sigma_{\text{DC}}}\right)^{-2} \rightarrow \frac{\sigma_{\text{DC}}}{\sigma_{\text{optical}}} = \text{f.o.m} \qquad (2)$$

with σ_{DC} representing the DC conductivity of the bulk material, σ_{optical} representing the optical conductivity, and R_s representing the sheet resistance of the film. According to the figure of merit model in Eq. (2), the films with small diameters exhibit a better performance (larger σ_{DC} values) than those with the larger diameters due to the higher film transparencies, despite higher nanowire concentrations that enable high conductivity. The present figure of merit model therefore suggests that smaller diameter nanowires with comparable lengths are better for use in transparent electrodes.

2.2.2 *Comparing haze factor to figure of merit*

Although electrode transparency and conductivity are important characteristics in high performance TCEs, the haze factor in a TCE of a solar cell is a critical contributor to the efficiency of the cell. Larger haze values correspond to increased scattering and hence an increased optical path length. The increased path length is of critical importance to thin-film devices where light trapping structures are needed to improve light absorption. To isolate the difference in haze factor in TCE films composed of relative small and large diameter Ag NWs, two separate vacuum-filtered thin film Ag NW samples were created from nanowire dispersions of small and large diameters. By altering the concentration of the nanowire dispersions, the transparency and sheet resistance for each film was controlled so as to achieve near equal values for relative small and large diameter Ag NW films. The haze factor of these films was measured by an integrating sphere setup, and is calculated as

$$\text{Haze\%} = \frac{T_2}{T_4} - \frac{T_2}{T_3} \tag{3}$$

The degree of forward scattering of the transmitted light by each film T_2 is divided by the total transmitted light through each film T_4 and then corrected for equipment bias T_1/T_3. The haze was calculated and compared for films of each diameter size in order to confirm which nanowire size best enhances forward scattering. The diameter rather than the length of the wires is the primary contributor to any differences

between them, because the nanowire length is approximately the same on average for both Ag NW dispersions.

The comparison of the transmittance curves and sheet resistance for films composed of relatively small and large diameters is given in Fig. 6. The transmittance curves of small diameter and large diameter Ag NW TCE films are nearly identical (the average deviation is 5.5%) as are the sheet resistances. According to current figure of merit models for TCE performance, these two Ag NW TCE films have nearly equal performances due to the similar transparency and conductivity characteristics. The haze factors of the films, however, are twice as large for the large diameter Ag NW TCE films as for the small diameter films. Despite nearly equal transparency and conductivity of the two film types, the TCE films consisting of Ag NWs with larger diameters prove to be better for solar cells due to their larger haze values. This observation opposes the generally accepted idea that increasing the aspect ratio by shrinking the nanowire diameters will produce a higher performing TCE in applications where a larger haze factor is preferred.

3 Conclusions

This study provides the first theoretical and experimental study of haze properties for Ag NWs, and also the first evidence that the current figure of merit for TCEs is insufficient to evaluate the performance of TCEs used in solar cell applications. According to the current models, transparency and conductivity
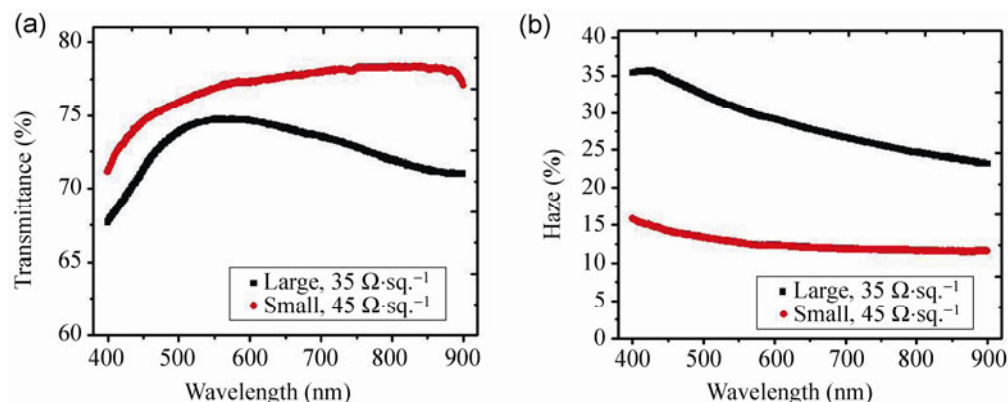

Figure 6 (a) Comparison of experimental transmittance data for a small diameter (~60 nm) Ag NW TCE film with R_s = 45 Ω/sq. and a large diameter (~150 nm) Ag NW TCE film with R_s = 35 Ω/sq. (b) Haze factor comparison between the same small diameter and large diameter Ag NW TCE films.

are the only properties significantly affecting the TCE performance. Although these properties are certainly important, haze factor is a critical property in TCEs for solar cells. This study demonstrates that the impact of haze factor is overlooked in films that contemporary figure of merit models would deem identical, and that the haze factor must be an independent variable to be included in new figure of merit formulas.

4   Experimental

Ag NW synthesis: Large diameter Ag NWs dispersed in ethanol were purchased commercially. Small diameter Ag NWs were synthesized by a slow titration method [23, 35]. In a typical synthesis, a mixture of 0.668 g of Polyvinylpropyline (PVP) and 0.022 g of KBr in 20 mL of ethylene glycol was heated to 170 °C for 20–30 min. The silver seeds were then introduced to the solution by adding 0.050 g of silver chloride (AgCl) into the solution. This was followed by a slow titration of the growth solution (0.220 g of silver nitrate (AgNO₃) in 10 mL of ethylene glycol) for 12–15 min. The titration of the AgNO₃ progressively stacks Ag⁺ ions onto the silver seeds, while the PVP restricts this stacking to anisotropic growth of a 1D nanowire, and the KBr salt precursor moderates the wire diameter to ensure long thin nanowires. The solution was maintained at 170 °C for an additional 30 min to complete the nanowire growth. The dispersion was then centrifuged three times with methanol at 6,000 rpm for 30 min each time to extract the nanowires from the dispersion.

TEM characterization: All TEM and HRTEM images were taken with a JEOL 2100F field emission transmission electron microscope (FE-TEM).

Thin film TCE fabrication: Transparent and conductive films were formed at room temperature from Ag NW dispersions with small diameters or large diameters through a vacuum filtration onto Anopore AAO substrates purchased from Anodisc. The filtered film was then transferred to a transparent PDMS substrate by pressing the PDMS against the filtered film, and then peeling the film off the AAO. Sheet resistance measurements were made with a four-point probe on the Ag NW films on PDMS.

Optical measurements: Optical haze and transmittance measurements of the Ag NW films transferred to PDMS substrates were recorded with a PerkinElmer Lambda 35 UV-vis spectrometer.

FDTD simulations: All FDTD simulations were designed and executed with Lumerical Solutions, Inc. software.

References

[1]   Bach, U.; Lupo, D.; Comte, P.; Moser, J. E.; Weissortel, F.; Salbeck, J.; Spreitzer, H.; Gratzel, M. Solid-state dye-sensitized mesoporous TiO₂ solar cells with high photon-to-electron conversion efficiencies. *Nature* **1998**, *395*, 583–585.

[2]   De, S.; Higgins, T. M.; Lyons, P. E.; Doherty, E. M.; Nimalraj, P. N.; Blau, W. J.; Boland, J. J.; Coleman, J. N. Silver nanowire networks as flexible, transparent, conducting films: Extremely high DC to optical conductivity ratios. *ACS Nano* **2009**, *3*, 1767–1774.

[3]   Kumar, A.; Zhou, C. The race to replace tin-doped indium oxide: Which material will win? *ACS Nano* **2010**, *4*, 11–14.

[4]   Gruner, G. Carbon nanotube films for transparent and plastic electronics. *J. Mater. Chem.* **2006**, *16*, 3533–3539.

[5]   Wu, Z.; Chen, Z.; Du, X.; Logan, J. M.; Sippel, J.; Nikolou, M.; Kamaras, K.; Reynolds, J. R.; Tanner, D. B.; Hebard, A. F.; Rinzler, A. G. Transparent conductive carbon nanotube films. *Science* **2004**, *305*, 1273–1276.

[6]   Zhang, M.; Fang, S.; Zakhidov, A. A.; Lee, S. B.; Aliev, A. E.; Williams, C. D.; Atkinson, K. R.; Baughman, R. H. Strong, transparent, multifunctional, carbon nanotube sheets. *Science* **2005**, *309*, 1215–1219.

[7] Hu, L.; Hecht, D. S.; Gruner, G. Percolation in transparent and conducting carbon nanotube networks. *Nano Lett.* **2004**, *4*, 2513–2517.

[8] Kim, K. S.; Zhao, Y.; Jang, H.; Lee, S. Y.; Kim, J. M.; Kim, K. S.; Ahn, J. H.; Kim, P.; Choi, J. Y.; Hong, B. H. Large-scale pattern growth of graphene films for stretchable transparent electrodes. *Nature* **2009**, *457*, 706–710.

[9] Geim, A. K.; Novoselov, K. S. The rise of graphene. *Nat. Mater.* **2007**, *6*, 183–191.

[10] Eda, G.; Fanchini, G.; Chhowalla, M. Large-area ultrathin films of reduced graphene oxide as a transparent and flexible material. *Nat. Nanotechnol.* **2008**, *3*, 270–274.

[11] Liu, C.-H.; Yu, X. Silver nanowire-based transparent, flexible, and conductive thin film. *Nanoscale Res. Lett.* **2011**, *6*, 75.

[12] Madaria, A. R.; Kumar, A.; Ishikawa, F. N.; Zhou, C. W. Uniform, highly conductive, and patterned transparent films of a percolating silver nanowire network on rigid and flexible substrates using a dry transfer technique. *Nano. Res.* **2010**, *3*, 564–573.

[13] Van de Groep, J.; Spinelli, P.; Polman, A. Transparent conducting silver nanowire networks. *Nano Lett.* **2012**, *12*, 3138–3144.

[14] Wu, H.; Hu, L. B.; Rowell, M. W.; Kong, D. S.; Cha, J. J.; McDonough, J. R.; Zhu, J.; Yang, Y. A.; McGehee, M. D.; Cui, Y. Electrospun metal nanofiber webs as high-performance transparent electrode. *Nano Lett.* **2010**, *10*, 4242–4248.

[15] Ebbesen, T. W.; Lezec, H. J.; Hiura, H.; Bennett, J. W.; Ghaemi, H. F.; Thio, T. Electrical conductivity of individual carbon nanotubes. *Nature* **1996**, *382*, 54–56.

[16] Hu, L. B.; Kim, H. S.; Lee, J. Y.; Peumans, P.; Cui, Y. Scalable coating and properties of transparent, flexible, silver nanowire electrodes. *ACS Nano* **2010**, *4*, 2955–2963.

[17] Rowell, M. W.; Topinka, M. A.; McGehee, M. D.; Prall, H. J.; Dennler, G.; Sariciftci, N. S.; Hu, L. B.; Gruner, G. Organic solar cells with carbon nanotube network electrodes. *Appl. Phys. Lett.* **2006**, *88*, 233506.

[18] Li, X. S.; Zhu, Y. W.; Cai, W. W.; Borysiak, M.; Han, B. Y.; Chen, D.; Piner, R. D.; Colombo, L.; Ruoff, R. S. Transfer of large-area graphene films for high-performance transparent conductive electrodes. *Nano Lett.* **2009**, *9*, 4359–4363.

[19] Hecht, D. S.; Hu, L. B.; Irvin, G. Emerging transparent electrodes based on thin films of carbon nanotubes, graphene, and metallic nanostructures. *Adv. Mater.* **2011**, *23*, 1482–1513.

[20] Kang, M. G.; Kim, M. S.; Kim, J. S.; Guo, L. J. Organic solar cells using nanoimprinted transparent metal electrodes. *Adv. Mater.* **2008**, *20*, 4408–4413.

[21] Lee, P.; Lee, J.; Lee, H.; Yeo, J.; Hong, S.; Nam, K. H.; Lee, D.; Lee, S. S.; Ko, S. H. Highly stretchable and highly conductive metal electrode by very long metal nanowire percolation network. *Adv. Mater.* **2012**, *24*, 3326–3332.

[22] Sun, Y. G. Silver nanowires-unique templates for functional nanostructures. *Nanoscale* **2010**, *2*, 1626–1642.

[23] Lee, J. Y.; Connor, S. T.; Cui, Y.; Peumans, P. Solution-processed metal nanowire mesh transparent electrodes. *Nano Lett.* **2008**, *8*, 689–692.

[24] Bergin, S. M.; Chen, Y. H.; Rathmell, A. R.; Charbonneau, P.; Li, Z. Y.; Wiley, B. J. The effect of nanowire length and diameter on the properties of transparent, conducting nanowire films. *Nanoscale* **2012**, *4*, 1996–2004.

[25] Yang, Y.; Wang, L.; Yan, H.; Jin, S.; Marks, T. J. Highly transparent and conductive double-layer oxide thin films as anodes for organic light-emitting diodes. *Appl. Phys. Lett.* **2006**, *89*, 051116.

[26] Muskens, O. L.; Rivas, J. G.; Algra, R. E.; Bakkers, E. P. A. M.; Lagendijk, A. Design of light scattering in nanowire materials for photovoltaic applications. *Nano Lett.* **2008**, *8*, 2638–2642.

[27] Van de Hulst, H. C. *Light Scattering by Small Particles*; John Wiley & Sons, Inc.: New York, 1957.

[28] Luk'yanchuk, B. S.; Tribelsky, M. I.; Ternovsky, V.; Wang, Z. B.; Hong, M. H.; Shi, L. P.; Chong, T. C. Peculiarities of light scattering by nanoparticles and nanowires near plasmon resonance frequencies in weakly dissipating materials. *J. Opt. A: Pure Appl. Opt.* **2007**, *9*, S294–S300.

[29] Oliva, J. M.; Gray, S. K. A computational study of the interaction of light with silver nanowires of different eccentricity. *Chem. Phys. Lett.* **2006**, *427*, 383–389.

[30] Giannini, V.; Sanchez-Gil, J. A. Calculations of light scattering from isolated and interacting metallic nanowires of arbitrary cross section by means of Green's theorem surface integral equations in parametric form. *J. Opt. Soc. Am. A* **2007**, *24*, 2822–2830.

[31] Catrysse, P. B.; Fan, S. H. Nanopatterned metallic films for use as transparent conductive electrodes in optoelectronic devices. *Nano Lett.* **2010**, *10*, 2944–2949.

[32] Spinelli, P.; Hebbink, M.; de Waele, R.; Black, L.; Lenzmann, F.; Polman, A. Optical impedance matching using coupled plasmonic nanoparticle arrays. *Nano Lett.* **2011**, *11*, 1760–1765.

[33] De, S.; King, P. J.; Lyons, P. E.; Khan, U.; Coleman, J. N. Size effects and the problem with percolation in nanostructured transparent conductors. *ACS Nano* **2010**, *4*, 7064–7072.

[34] Critchley, K.; Khanal, B. P.; Górzny, M. L.; Vigderman, L.; Evans, S. D.; Zubarev, E. R.; Kotov, N. A. Near-bulk conductivity of gold nanowires as nanoscale interconnects and the role of atomically smooth interface. *Adv. Mater.* **2010**, *22*, 2338–2342.

[35] Xia, Y. N.; Yang, P. D.; Sun, Y. G.; Wu, Y. Y.; Mayers, B.; Gates, B.; Yin, Y. D.; Kim, F.; Yan, Y. Q.; One-dimensional nanostructures: Synthesis, characterization, and applications. *Adv. Mater.* **2003**, *15*, 353–389.